Application of 3D MoM/CBFM Technique to the Problem of Electromagnetic Scattering by Complex-Shaped Precipitation Particles

Ines Fenni*, Ziad S. Haddad*, Hélène Roussel, Raj Mittra#**

*** Jet Propulsion Laboratory, USA ** UPMC Univ Paris 06, France, # EMC Lab , University of Central Florida, USA**

National Aeronautics and Space Administration

I – Introduction :

We apply a powerful domain decomposition technique, known as the Characteristic Basis Function Method (CBFM), to the problem of EM scattering by complex-shaped particles, and this, in the context of a 3D full-wave model based on the volume-integral equation formulation of the electric fields. We so take advantage of the high computational efficiency of the CBFM and its associated good level of accuracy when modeling the problem of EM scattering by complex-shaped precipitation particles.

II – Application of the CBFM to the problem of scattering by complex particles :

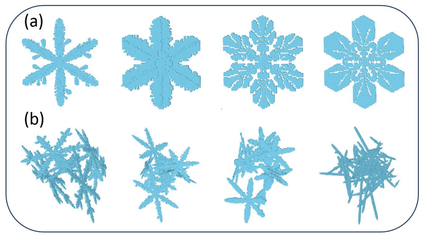

Pristine crystals **(a)** simulated using the snowflake algorithm [1] and aggregate snow particles **(b)**

3D full-wave model based on the use of the **volume integral equation method (VIEM)** with **piecewise constant basis functions.**
The model is applied here to pristine ice crystals and aggregate snow particles simulated by Kuo et al [1] using a 3D growth model pioneered by Gravner and Griffeath [2]

Frequencies of interest : (35 - 380 GHz)

Integral representation of the total electric field (EFIE) :

$$\bar{E}(\bar{r}) = \bar{E}^i(\bar{r}) + \left(k_0^2 + \nabla\nabla.\right) \int_\Omega \chi(\bar{r}')\, G(\bar{r},\bar{r}')\, \bar{E}(\bar{r}')\, d\bar{r}'$$

where $\bar{E}(\bar{r})$ is the field inside the scatterer, $\bar{E}^i(\bar{r})$ is the incident field, $\chi(\bar{r}')$ is the dielectric contrast at the location r', k_0 is the wavenumber in air and $G(\bar{r},\bar{r}')$ is the free space Green's function. We rewrite the integral equation above as :

$$\Gamma\bar{E}(\bar{r}) = \bar{E}^i(\bar{r}) \quad \text{where} \quad \Gamma = \underline{I} - \left(k_0^2 + \nabla\nabla.\right) \int_\Omega \chi(\bar{r}')\, G(\bar{r},\bar{r}')\, d\bar{r}'$$

Application of a Method of Moments (MoM) :

The particle is discretized into **N** cubic cells Ω_n ,of side c_n, small enough to consider that the field inside is constant

$$c_n = \frac{\lambda_s}{10} \; ; \; \lambda_s = \frac{\lambda_0}{\sqrt{Re(\varepsilon_r)}}$$

$$\bar{E}(\bar{r}) = \sum_{n=1}^{N}\sum_{q=1}^{3} E_q^n\, \bar{F}_q^n(\bar{r})$$

where E_q^n is the constant unknown of $\bar{F}_q^n$, the nth basis function for the component (q = x, y or z) of the field inside the particle

To select a set of test functions W_p^m(m=1,..,M and p= x, y, z), the **point matching** method is used. So, M=N and W_p^m is a Dirac delta function concentrated at the center of the cell Ω_n

$$\Gamma\bar{E}(\bar{r}) = \bar{E}^i(\bar{r}) \quad \Rightarrow \quad \sum_{n=1}^{N}\sum_{q=1}^{3} \langle \bar{W}_p^m, \Gamma\bar{F}_q^n \rangle E_q^n = \langle \bar{W}_p^m, \bar{E}^i \rangle$$

where $\bar{F}_q^n(\bar{r}) = \begin{Bmatrix} \mathbf{1}; & \bar{r} \in \Omega_n \\ \mathbf{0}; & \bar{r} \notin \Omega_n \end{Bmatrix} \hat{q}$

and $\bar{W}_p^m(\bar{r}) = \delta(\bar{r} - \bar{r}_m)\, \hat{p}$

Z is the 3N x 3N full matrix representing the interactions between the cells composing the particle. E^i is the incident field of size 3N and E is the unknown solution vector of size 3N that represents the total electric field inside the particle in the x, y and z directions.

$$\sum_{n=1}^{N}\sum_{q=1}^{3} Z_{pq}^{mn} E_q^n = E_p^{i,m} \quad \Rightarrow \quad \boldsymbol{Z\,E = E^i}$$

The elements of $\underline{Z} = [Z_{pq}^{mn}]$ are given by $Z_{pq}^{mn} = \delta_{mn}\delta_{pq} - Z_{pq}^{s,mn}$ where

$$Z_{pq}^{s,mn} = k_0^2 \int_{\Omega_n} \chi(\bar{r}'_n)\, G_{pq}^s(\bar{r}_m,\bar{r}'_n)\, d\bar{r}'_n + \sum_{q=1}^{3} \frac{\partial^2}{\partial p_m \partial q_m} \int_{\Omega_n} \chi(\bar{r}'_n)\, G_{pq}^s(\bar{r}_m,\bar{r}'_n)\, d\bar{r}'_n$$

If m = n, in order to avoid singularities, $Z_{pq}^{s,mn}$ is computed using Hadamard regularization. Then the integral on Ω_n is approximated by an integral on sphere of radius $a_n = c_n\sqrt[3]{3/(4\pi)}$

if m = n : $Z_{pq}^{s,mn} = \mathcal{H}\left(\int_{\Omega_n} \left(k_0^2 + \frac{\partial^2}{\partial p_m^2} \right) G_{pq}^s(\bar{r}_m,\bar{r}'_n)\, d\bar{r}'_n \right) \chi_n$ if p = q ; 0 if p ≠ q

$$= \frac{2}{3}\, e^{jk_0a_n}(1 - jk_0a_n) - 1$$

if m ≠ n : $\int_{\Omega_n} G_{pq}^s(\bar{r}_m,\bar{r}'_n)d\bar{r}'_n = 4\pi \times \frac{\sin(k_0a_n) - k_0a_n\cos(k_0a_n)}{k_0^3} \times G_{pq}^s(\bar{r}_m,\bar{r}'_n)$

Application of the Characteristic Basis Function Method :

As well known, the VIEM is limited by its heavy computational burden, which scales as O[(3N)^2]. To overcome this burden, we employ the CBFM which has been proven to be accurate and efficient when applied to large-scale EM problems, even when the computational resources are limited.

- ❖ **B**etter adapted to multiple right-hand side problem
- ❖ **H**ighly amenable to MPI parallelization
- ❖ **S**ubject to a wide variety of enhancement techniques
- ❖ **A**daptable to the needs of the user (memory or CPU time) through h_B

After dividing the 3D complex geometry of the precipitation particle of **N** cells into **M blocks** of height $\mathbf{h_B}$, the **CBFM** procedure [2] consists in generating $\mathbf{S_i}$ Characteristic Basis Functions (CBFs) for each block **i** in order to generate a final reduced matrix of size **K x K** where **K = Sum (S_1, S_2, … S_M)**. This results in a substantial size-reduction of the MoM matrix and enables us to use of a direct method for its inversion.

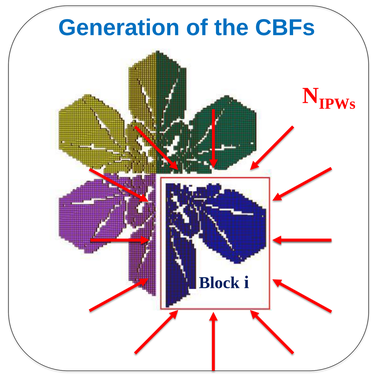

$$\begin{pmatrix} E_1^{(i,\theta_1,\varphi_1)} & E_1^{(i,\theta_2,\varphi_1)} & \dots & E_1^{(i,\theta_{N\theta},\varphi_{N\varphi})} \\ E_2^{(i,\theta_1,\varphi_1)} & E_2^{(i,\theta_2,\varphi_1)} & \dots & E_2^{(i,\theta_{N\theta},\varphi_{N\varphi})} \\ E_3^{(i,\theta_1,\varphi_1)} & E_3^{(i,\theta_2,\varphi_1)} & \dots & E_3^{(i,\theta_{N\theta},\varphi_{N\varphi})} \\ \vdots & \vdots & \ddots & \vdots \\ E_{N_i}^{(i,\theta_1,\varphi_1)} & E_{N_i}^{(i,\theta_2,\varphi_1)} & \dots & E_{N_i}^{(i,\theta_{N\theta},\varphi_{N\varphi})} \end{pmatrix}$$

(N_{IPWs} columns)

Singular Value Decomposition (SVD) + thresholding (% σ_1*10^{-3})

S_i CBFs for the block i

Direct solver

By storing and solving the resulting reduced system of equations, instead of the original one, we are able to achieve a significant gain both in terms of CPU time and required memory.

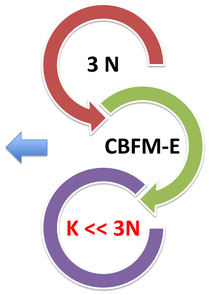

Computation of Z^c

Example : M = 4

$$Z^c = \begin{pmatrix} C^{(1)t} Z_{11} C^{(1)} & \dots & C^{(1)t} Z_{14} C^{(4)} \\ C^{(2)t} Z_{21} C^{(1)} & \dots & C^{(2)t} Z_{24} C^{(4)} \\ \vdots & \ddots & \vdots \\ C^{(4)t} Z_{41} C^{(1)} & \dots & C^{(4)t} Z_{44} C^{(4)} \end{pmatrix}$$

K = S_1 + S_2 + S_3 + S_4 << 3*N

Compression Rate

$$ICR\,(\%) = 100 \times \frac{size\ of\ Z^c}{size\ of\ Z^{MoM}}$$

Enhancement mo are employed to substantially reduce the CPU time needed to compute the CBFs and to generate the reduced matrix Z^c or to increase the compression rate achieved by the CBFM.

1. Diagonal representation of the MBFs

($3N_i$)^3 $E_i^{(\theta,\varphi)} = Z_{ii}^{-1}\, E_i^{ref,(\theta,\varphi)}$

$3N_i$ $\tilde{E}_i^{(\theta,\varphi)} = \dfrac{E_i^{ref,(\theta,\varphi)}}{Z_{ii}}$

2. Use of the ACA to speed-up the generation of Z^c

$Z_{i,j}^c \approx \langle C^{(i)t}, \tilde{Z}_{i,j}^{MoM}\, C^{(j)} \rangle$

where $\tilde{Z}_{i,j}^{MoM} = U_i^{3N_i \times r}\, V_j^{r \times 3N_j}$

and **r** (effective rank of $\mathbf{Z_{i,j}}^{\mathbf{MoM}}$) << 3 N_i and 3 N_j

3. Multilevel scheme of the CBFM

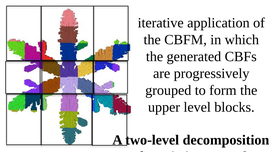

iterative application of the CBFM, in which the generated CBFs are progressively grouped to form the upper level blocks.

A two-level decomposition of a pristine crystal.

III – Numerical results :

We compute the **extinction, absorption, scattering and back-scattering efficiency factors Q_{ext} = $C_{ext}/\pi a^2$, Q_{abs} = $C_{abs}/\pi a^2$, Q_{scat}=$C_{scat}/\pi a^2$** and **Q_{bks}=C_{bks} /πa^2** as functions of x = ka=2πa/λ, and compares the results with those derived from the Mie series (spherical particle) and with those calculated using Discrete Dipole Approximation as coded in DDSCAT 7.1.

For each incident direction (θ_i,φ_i), C_{ext} , C_{scat} and C_{bks} are derived from the **scattering matrix S** as follow

$$C_{ext} = \frac{2\pi}{k^2}\left[Re\{S_{VV}(\theta_{fwd},\varphi_{fwd})\} + Re\{S_{HH}(\theta_{fwd},\varphi_{fwd})\}\right]$$

$$C_{scat} = \frac{1}{2k^2}\int_0^{2\pi}\int_0^{\pi} [S_{VV}(\theta_s,\varphi_s)^2 + S_{VH}(\theta_s,\varphi_s)^2 + S_{HV}(\theta_s,\varphi_s)^2 + S_{HH}(\theta_s,\varphi_s)^2]\sin(\theta)\, d\theta\, d\phi$$

$$C_{bks} = \frac{1}{2k^2}[S_{VV}(\theta_{bks},\varphi_{bks})^2 + S_{VH}(\theta_{bks},\varphi_{bks})^2 + S_{HV}(\theta_{bks},\varphi_{bks})^2 + S_{HH}(\theta_{bks},\varphi_{bks})^2]$$

where (θ_s,φ_s) describes the scattering direction and $(\theta_{fwd}, \varphi_{fwd})$ and $(\theta_{bks}, \varphi_{bks})$ refers respectively to the scattering forward direction and backscattering direction

Single incident direction/target orientation:

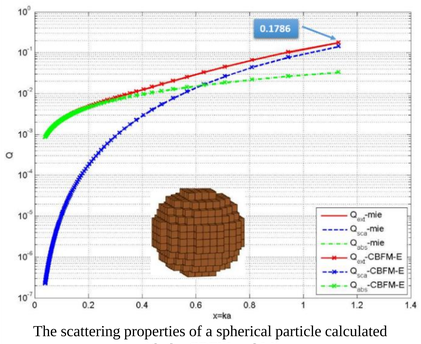

The scattering properties of a spherical particle calculated with the CBFM and Mie

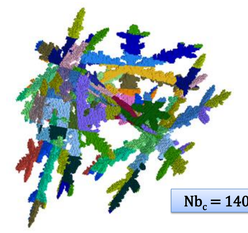

As we can see below, applied to a numerically large particle, the OpenMP CBFM code overtake the OpenMP DDScat code in terms of CPU time even for a single incident beam (for CBFM) / target orientation (for DDScat)

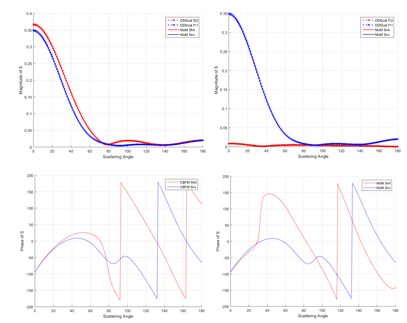

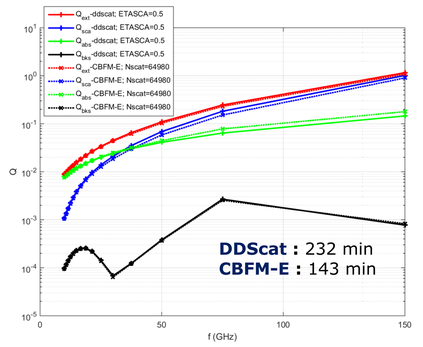

The scattering properties of an aggregate snow particle of effective radius a_p=1.614 mm (max. dim. = 11.45 mm) calculated using the MoM/CBFM-E and DDScat

Orientational Averaging over incident directions:

The angular averages are accomplished by evaluating the scattering quantities (f =Q_{ext} or Q_{sca} or Q_{bks}) for selected incident directions (θ_i; φ_i).

$$\langle f \rangle = \frac{1}{4\pi}\int_0^{\pi}\int_0^{2\pi} f(\theta i, \varphi i)\sin\theta i\; d\theta i\, d\varphi i$$

Combined to **a direct solver-based method**, this enables us to overcome one major drawback of DDScat coming from the fact that if orientation averages are needed then computationally greedy linear equations must be **solved repeatedly**.

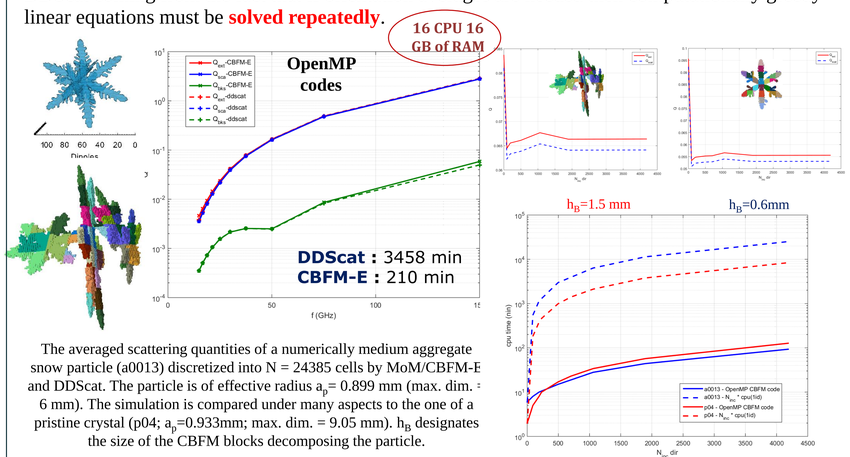

The averaged scattering quantities of a numerically medium aggregate snow particle (a0013) discretized into N = 24385 cells by MoM/CBFM-E and DDScat. The particle is of effective radius a_p= 0.899 mm (max. dim. = 6 mm). The simulation is compared under many aspects to the one of a pristine crystal (p04; a_p=0.933mm; max. dim. = 9.05 mm). h_B designates the size of the CBFM blocks decomposing the particle.

References : [1] Kuo, K. S., Olson, W. S., Johnson, B. T., Grecu, M., Tian, L., Clune, T. L., ... & Meneghini, R. (2016). The Microwave Radiative Properties of Falling Snow Derived from Nonspherical Ice Particle Models. Part I: An Extensive Database of Simulated Pristine Crystals and Aggregate Particles, and Their Scattering Properties. Journal of Applied Meteorology and Climatology, 55(3), 691-708. [2] E. Lucente, G. Tiberi, A. Monorchio, and R. Mittra, "An iteration-free MoM Approach Based on Excitation Independent Characteristic Basis Functions for Solving Large Multiscale Electromagnetic Scattering Problems", IEEE Trans. Antennas Propag., Vol. 56, no. 4, pp.999-1007, Apr. 2008.